

# An Adaptive Procedure for the Limit Analysis of FRP Reinforced Masonry Vaults and Applications

<sup>1</sup>Andrea Chiozzi, <sup>2</sup>Gabriele Milani, <sup>1</sup>Nicola Grillanda and <sup>1</sup>Antonio Tralli

<sup>1</sup>Department of Engineering, University of Ferrara, Via Saragat 1, 44122 - Ferrara, Italy

<sup>2</sup>Department of Architecture, Built Environment and Construction Engineering (A.B.C.), Technical University of Milan, Piazza Leonardo da Vinci 32, 20133 - Milan, Italy

## Article history

Received: 29-8-2016

Revised: 4-10-2016

Accepted: 5-10-2016

Corresponding Author:

Andrea Chiozzi

Department of Engineering,  
University of Ferrara, Ferrara,  
Italy

Email: andrea.chiozzi@unife.it

**Abstract:** The present paper discusses an adaptive procedure for the kinematic limit analysis of FRP reinforced masonry vaults through applications. The approach relies on a new Genetic Algorithm NURBS-based general framework, which has been recently presented by the authors. The basic idea consists into exploiting the NURBS structure of a CAD geometric 3D model of the selected reinforced masonry vault, in order to define an adaptive rigid body assembly on which an (upper bound) limit analysis can be performed. Internal dissipation is allowed exclusively along element interfaces. A Genetic Algorithm is used to adjust the initial assembly, until element edges accurately approximate the actual collapse mechanism. A number of structural examples are provided and discussed, showing that the approach can be a very useful tool for the structural design and assessment of FRP reinforced masonry vaults.

**Keywords:** FRP, Masonry, Limit Analysis, NURBS

## Introduction

Masonry vaults are one of the most common structural types in the historical constructions of both ancient and modern architecture. Consequently, the search for new techniques for their preservation is still an open issue, which is growing over time along with the need for new efficient tools to evaluate their load-bearing capacity. Moreover, as witnessed by the many recent seismic events, another critical issue is the insufficient performance of curved masonry structures under the action of earthquakes, particularly in the case of historical buildings and inadequate modern constructions. While conventional retrofitting techniques, like for example external reinforcement with steel plates or reinforced concrete overlays, have been proven present serious drawbacks (they are expensive, often impractical and add considerable mass to the structure), in the last decades the use of Fiber-Reinforced Polymer (FRP) strips for reinforcing masonry structures has become very well-received (Corradi *et al.*, 2002). Due to their high mechanical strength, chemical stability, low weight and availability in plenty of different shapes, CFRPs can be favorably applied at the intrados or extrados of flat and curved masonry shells (i.e. walls, arches and vaults) in order to prevent collapse mechanisms, therefore increasing the overall safety factor.

Existing computational methods for the structural analysis of masonry vaults can be categorized into two broad classes: the Finite Element methods developed both for nonlinear incremental analysis (Milani and Tralli, 2012) and for limit analysis (Milani *et al.*, 2008; 2009) and the thrust network methods (Block *et al.*, 2006). Practical application of these procedures requires skilled users and, for thrust network methods, the definition of an equilibrium surface for the vault, which is a priori unknown.

The authors have recently proposed a new adaptive NURBS-based approach (Chiozzi *et al.*, 2016a) for the limit analysis of masonry vaults based on an upper bound formulation also allowing for the presence of FRP reinforcements (Chiozzi *et al.*, 2016b; 2016c) NURBS (i.e. Non-Rational Uniform Bi-Spline) are special approximating base functions widely used in the field of 3D modeling (Cottrell *et al.*, 2009). A given FRP reinforced vault geometry can be represented by NURBS parametric surfaces for both masonry and reinforcement, which can be generated within any commercial free form modeler. A mesh of the given surfaces, still providing an exact representation of the vaulted surface and of reinforcement, can be obtained by making use of NURBS functions properties. Each element of the mesh is a NURBS surface itself and is assumed as a rigid body.

An upper bound limit analysis formulation is devised for the obtained rigid body assembly, which accounts for

the main aspects of masonry material and in which dissipation is allowed along element edges only. Moreover, a Genetic Algorithm adaptive procedure is implemented which allows to adjust the initial NURBS assembly until a good estimate of the collapse load multiplier is obtained, i.e. when element edges accurately approximate the actual failure mechanism. The strength of the proposed method lies in the fact that even by using a mesh made of very few elements, it is possible to obtain an accurate estimate of the load multiplier, thus exhibiting an edge over existing methods for the collapse analysis of masonry vaults in terms of computational efficiency.

This paper is devoted to give a more in-depth insight into the effectiveness of the proposed methodology as a design tool for the prediction of the actual failure mechanisms and load bearing capacity of FRP masonry vaulted structures of arbitrary shape. To this aim, new structural examples have been analyzed and discussed.

The paper is organized as follows: in Section 2 a synthetic survey of the GA-NURBS approach is given. In Section 3, the procedure is exemplified and validated by considering several new structural examples. In Section 4, conclusions are drawn and future research directions are given.

## The GA-NURBS Approach: A Quick Overview

The GA-NURBS limit analysis procedure can be split into three main steps: geometry modeling of the FRP reinforced vault and definition of a rigid block assembly, kinematic limit analysis through linear programming and mesh adaptation through a Genetic Algorithm. A summary of the procedure is hereby proposed. The reader is addressed to (Chiozzi *et al.*, 2016c) for more details.

### From 3D Model to Structural Rigid Block Assembly

FRP reinforced masonry vaults can be represented in any free form 3D modeler using NURBS surfaces for both FRP strips and the mean surface of the underlying vault. NURBS basis functions are built upon B-splines basis functions, i.e. piecewise polynomial functions  $N_{i,p}$  defined by a sequence of coordinates  $\Xi = \{\xi_1, \xi_2, \dots, \xi_{n+p+1}\}$ , also known as the knot vector, where the so-called knots,  $\xi_i \in [0,1]$ , are points in a parametric domain, in which  $p$  and  $n$  denote the polynomial order and the total number of basis functions, respectively. Given a set of weights,  $w_i \in \mathbb{R}$ , the NURBS basis functions,  $R_{i,p}$ , read:

$$R_{i,p}(\xi) = \frac{N_{i,p}(\xi)w_i}{\sum_{i=1}^n N_{i,p}(\xi)w_i} \quad (1)$$

Geometries that can be generated with B-spline and NURBS are obtained as linear combinations of basis functions (Cottrell *et al.*, 2009). In particular, a NURBS surface of degree  $p$  in the  $u$ -direction and  $q$  in the  $v$ -direction is a parametric surface in the three-dimensional Euclidean space defined as:

$$S(u,v) = \sum_{i=0}^n \sum_{j=0}^m R_{i,j}(u,v)B_{i,j} \quad (2)$$

where,  $\{B_{ij}\}$  form a bidirectional net of control points. Given a NURBS surface  $S(u,v)$ , isoparametric curves on the surface can be defined by fixing one parameter in the parameter space and letting the other vary. By fixing  $u = u_0$  the isoparametric curve  $S(u_0, v)$  is defined on the surface  $S$ , whereas by fixing  $v = v_0$  the isoparametric curve  $S(u, v_0)$  is obtained. Many commercial free form surface modelers, such as Rhinoceros® (McNeel, 2008), utilize NURBS representation and its properties to generate and manipulate surfaces in the three-dimensional space. In the numerical simulations contained in Section 3, both vault mid-surfaces and FRP strips have been modeled within Rhinoceros as NURBS surfaces and the resulting NURBS structure have been imported within a MATLAB® environment through the IGES (Initial Graphics Exchange Specification) standard (USPRO, 1996) following an idea proposed by some of the authors in (Chiozzi *et al.*, 2015) for masonry arches.

Once the NURBS structure created within Rhinoceros® has been transferred to the MATLAB® environment, it is possible to manipulate it by exploiting NURBS properties in order to define a NURBS mesh of the masonry mid-surface, in which each element is a NURBS surface itself. Furthermore, it is possible to model vault thickness at each interface between elements by offsetting the original interface inward and outward through a translation in the direction normal to the NURBS surface. Typically, the easiest way to generate a NURBS mesh on a given surface is to define a subdivision of the two-dimensional parameters space  $u-v$ , which follows from subdividing the knot vectors in both  $u$  and  $v$  directions into equal intervals. The resulting mesh is defined by isoparametric curves on the surface in the three-dimensional Euclidean space. Each element of the mesh is a NURBS surface and its edges are branches of isoparametric curves belonging to the initial surface. More in general, different meshes of the NURBS surface can be obtained for arbitrary partitions of the parameters space into quadrilateral or triangular domains. For each element of the mesh,  $E_i$ , integral quantities like area and position of the center of mass can be numerically evaluated by adopting an isoparametric approach coupled with a 3-point standard Gauss quadrature rule.

### Kinematic Limit Analysis

Starting from the geometrical properties of each element of the assembly, an upper bound formulation of limit analysis can be outlined. Since elements are considered rigid, internal dissipation is allowed only at the interfaces between adjoining elements in the proposed model. Be  $N_E$  the number of elements composing the NURBS mesh, which geometrically represents the FRP reinforced vaulted surface. Since each element is considered as a rigid element, the kinematics of each element is determined by the six generalized velocity components  $\{u_x^i, u_y^i, u_z^i, \Phi_x^i, \Phi_y^i, \Phi_z^i\}$  of its center of mass  $G_i$ , expressed in a global reference system  $Oxyz$ . On the structure, dead loads  $F_0$  and live loads  $\Gamma$  are acting. Three types of interfaces can be recognized: *masonry-masonry*, *FRP-masonry* and *FRP-FRP* interfaces. Indicating by  $N_I^{TOT} = N_I^{M-M} + N_I^{M-F} + N_I^{F-F}$  the total number of interfaces, total internal dissipation power  $D_{int}$  is equal to the sum of the power dissipated along each interface  $P_{int}^i$ . Furthermore, total internal dissipation power  $D_{int}$  is equal to the sum of the powers of live ( $1.\Gamma$ ) and dead ( $F_0$ ) loads, indicated as  $P_\Gamma$  and  $P_{F_0}$  respectively:

$$D_{int} = \sum_{i=1}^{N_I} P_{int}^i = P_\Gamma + P_{F_0} \quad (3)$$

$\Gamma$  is a load multiplier. The linear programming problem related to the kinematic formulation of limit analysis consists in an appropriate minimization of the load multiplier  $\Gamma$  under the action of suitable constraints, which are quickly described in the following Subsections. The vector of unknowns of the linear programming problem,  $X$ , contains the six generalized velocity components for each element and a number of plastic multipliers defined on each interface.

### Geometric Constraints

Vertex belonging to element free edges can be subjected to external kinematic constraints, by imposing an assigned value for translational and/or rotational velocities at these points. For each of such vertex  $V_j$ , kinematic constraints can be expressed in terms of generalized velocities of the center of mass of the  $i$ -th element they belong. In general, all linear geometric constraints can be re-written in the following standard form:

$$A_{eq,geom} X = b_{eq,geom} \quad (4)$$

where,  $A_{eq,geom}$  is the matrix of geometric constraints and  $b_{eq,geom}$  the corresponding vector of coefficients.

### Compatibility Constraints

#### Masonry-Masonry Interfaces

Intrados and extrados edges of each interface have been subdivided into an assigned number ( $N_{sd}^M + 1$ ) of points. On each point  $P_i$  of each interface, which separates the two elements  $E'$  and  $E''$ , the following compatibility equation must hold:

$$\Delta \tilde{u} = \dot{\lambda} \frac{\partial f}{\partial \sigma} \quad (5)$$

where,  $\sigma = [\sigma_{mm}, \sigma_{ms}, \sigma_{mi}]$  is the stress vector acting on  $P_i$  in the three local reference directions,  $f(\sigma)$  is a suitable yield function and  $\dot{\lambda}$  is an unknown plastic multiplier vector. In Equation  $\Delta \tilde{u}$  is the representation in the local reference system of the quantity  $\Delta u$  in the global reference system which is defined as:

$$\Delta u = u'_{p_i} - u''_{p_i} \quad (6)$$

where,  $u'_{p_i}$  is the vector composed by the three translational velocity components of the point  $P_i$  seen as belonging to element  $E'$  and  $u''_{p_i}$ . The yield surface  $f(\sigma)$  have been obtained by means of a homogenization procedure based on the so-called Method of Cells (MoC), in order to account for different disposition of brick courses. With an iterative solution it is possible to easily provide a linearization for the assigned yield surface  $f(\sigma)$ . Let us indicate with the equation  $A_i \sigma_{mm} + B_i \sigma_{ms} + C_i \sigma_{mi} = 1$  the  $i$ -th plane representing  $f(\sigma)$ . In such a way Equation simplifies to the equation:

$$\Delta \tilde{u} = \begin{bmatrix} \sum_{i=1}^{N^{pl}} A_i \dot{\lambda}^i \\ \sum_{i=1}^{N^{pl}} B_i \dot{\lambda}^i \\ \sum_{i=1}^{N^{pl}} C_i \dot{\lambda}^i \end{bmatrix} \quad (7)$$

where,  $\dot{\lambda}^i$  is the  $i$ -th plane plastic multiplier and  $N^{pl}$  is the total number of linearization planes used.

The previous constraint must hold for each point  $P_i$  of each interface.

#### FRP-FRP Interfaces

FRP elements are supposed infinitely rigid. Therefore, plastic dissipation is allowed only at the interfaces between contiguous elements due to stresses acting in the fibers direction. Again, FRP-FRP interface can be subdivided into an assigned number ( $N_{sd}^F + 1$ ) of

points  $P_i$ . Continuity of the velocity field is imposed at each interface between contiguous FRP only along local transversal and normal directions, whereas a possible jump of velocities is admitted along the longitudinal direction. Different limit stresses are assumed in tension and compression, namely  $f_{FRP}^+$  (assumed equal to  $f_{jdd}$  or  $f_{jdd,rid}$  in agreement with (CNR-DT200, 2013), see the following section for details) for tensile failure and  $f_{FRP}^- \approx 0$  for compression buckling respectively. To be kinematically admissible, velocity jump at the interfaces must comply to the following equality constraints which particularize the associated flow rule:

$$\Delta \tilde{u} \begin{bmatrix} \Delta \tilde{u}_n \\ \Delta \tilde{u}_t \\ \Delta \tilde{u}_s \end{bmatrix} = \begin{bmatrix} \lambda_i^{I-FRP+} - \lambda_i^{I-FRP-} \\ 0 \\ 0 \end{bmatrix} \quad (8)$$

where,  $\lambda_i^{I-FRP+}$  and  $\lambda_i^{I-FRP-}$  are plastic multiplier rates of point  $P_i$  on the FRP-FRP interface corresponding to  $f_{FRP}^+$  and  $f_{FRP}^-$  respectively.

#### FRP-Masonry Interfaces

One of the paramount aspects in the application of composite materials for retrofitting structural elements is the adhesion between the reinforcement and the underlying material. As suggested in the in the Italian technical norm (CNR-DT200, 2013), a simplified approach to evaluate the delamination phenomenon, is to suitably limit force action on the FRP strip. In particular, the  $f_{jdd}$  design tensile strength of FRP elements, which is used in the former Subsection, is given by the relation:

$$f_{jdd} = \frac{1}{\gamma_{fd} \sqrt{\gamma_M}} \sqrt{\frac{2 \cdot E_{FRP} \cdot \Gamma_{Fk}}{t_{FRP}}} \quad (9)$$

If the so called bond length  $l_b$  is greater than the optimal bond length  $l_e$  or:

$$f_{jdd,rid} = f_{jdd} \frac{l_b}{l_e} \left( 2 - \frac{l_b}{l_e} \right) \quad (10)$$

if  $l_b \leq l_e$ . In equations and the following symbols have been used:  $f_{jdd,rid}$ , the reduced value of the design bond strength;  $f_{jdd}$ , the design bond strength;  $E_{FRP}$ , the FRP Young modulus;  $t_{FRP}$ , the FRP thickness;  $\gamma_{fd}$ , a safety factor (assumed equal to 1.20);  $\gamma_M$ , partial safety factor for masonry (assumed equal to 1.0);  $l_b$ , the bond length of FRP elements;  $l_e$ , the optimal bond length of FRP corresponding to the minimal bond length able to bear the maximum anchorage force ( $f_{mim}$  is masonry average tensile strength). Finally,  $\Gamma_{Fk}$  represents the characteristic value of the specific fracture energy of the FRP reinforced masonry upon delamination.

In order to take into account dissipation along the FRP-masonry interface, an assigned number  $N_p^{M-F}$  of Gauss points have been fixed on the FRP-masonry interface surface. As for masonry-masonry interfaces, a linearization of FRP-masonry failure surface (provided by the Italian norm) in the form  $A_k \tau_{sl} + B_k \tau_{ti} + C_k \sigma_{ni} = D_k$ ,  $k = 1, \dots, N_{PL}^{M-F}$  ( $N_{PL}^{M-F}$  is the number of planes used in the linearization of the failure surface) is assumed. In the framework of associated limit analysis, the following equality constraints must be imposed, which particularize the associate flow rule:

$$[u_i] = \begin{bmatrix} \Delta u_s^i \\ \Delta u_t^i \\ \Delta u_n^i \end{bmatrix} = \begin{bmatrix} \sum_{k=1}^{N_{PL}^{M-F}} A_k \dot{\lambda}_i^{M-F,k} \\ \sum_{k=1}^{N_{PL}^{M-F}} B_k \dot{\lambda}_i^{M-F,k} \\ \sum_{k=1}^{N_{PL}^{M-F}} C_k \dot{\lambda}_i^{M-F,k} \end{bmatrix} \quad (11)$$

where,  $i = A, B$  or  $C$ ,  $\dot{\lambda}_i^{M-F,k}$  is the k-th plastic multiplier rate corresponding to the k-th plane.

#### Further Necessary Conditions

Plastic multipliers must be positive or equal to zero:

$$\dot{\lambda}_{ij} \geq 0 \quad (12)$$

Finally, normality condition must be enforced:

$$P_{\Gamma=1} = 1 \quad (13)$$

#### The Linear Programming Problem

Remembering Equation and following the kinematic theorem of limit analysis, the related linear programming problem can be stated as follows:

$$\min \left\{ \sum_{i=1}^{N_i} P_{int}^i - P_{F_0} \right\} \quad (14)$$

under geometric constraints, compatibility constraints, Eq. 12 and Eq. 13. The unknowns of the linear programming problem are the  $6 \cdot N_E$  generalized velocity components of the center of mass of each element and the total number of plastic multipliers at each point of each interface.

#### Adapting the Rigid Body Assembly: The Genetic Algorithm

It is necessary to introduce an algorithm which allows to adjust the assembly in order to find the minimum collapse multiplier among all possible configurations and therefore to determine the actual

collapse mechanism. A genetic algorithm is a method for solving both constrained and unconstrained optimization problems based on a natural selection process that mimics biological evolution of individuals. A NURBS mesh of a vaulted surface, is determined by a given number  $N_{par}$  of real parameters  $p_1, p_2, \dots, p_{N_{par}}$ , that depend on the type of collapse mechanism which must be detected. A given NURBS mesh is regarded as an individual and each individual, is written as an array with  $1 \times N_{par}$  elements:

$$individual = [p_1, p_2, \dots, p_{N_{par}}] \quad (15)$$

Each individual has a cost, found by evaluating a cost function  $f$  at the parameters  $p_1, p_2, \dots, p_{N_{par}}$ . The cost function  $f$  is defined as a function which outputs the collapse load multiplier  $\lambda_c$  for every assigned individual (i.e. an assigned mesh on the surface) through the implementation of the limit analysis procedure described:

$$\lambda_c = f(individual) = f(p_1, p_2, \dots, p_{N_{par}}) \quad (16)$$

To begin the genetic algorithm, we define an initial population of  $N_{ipop}$  individuals. A matrix represents the population with each row in the matrix being a  $1 \times N_{par}$  array (individual) of continuous parameters values. Given an initial population of  $N_{ipop}$  individuals, the full matrix of  $N_{ipop} \times N_{par}$  random values is generated by:

$$IPOP = (hi - lo) \times random\{N_{ipop}, N_{par}\} + lo \quad (17)$$

where,  $random\{N_{ipop}, N_{par}\}$  is a function that generates an  $N_{ipop} \times N_{par}$  matrix of uniform random numbers,  $hi$  and  $lo$  are the highest and lowest number in the parameter range. Individuals are not all "create equal": each one's worth is assessed by the cost function. In order to decide which chromosomes in the initial population of individuals are fit enough to survive and reproduce offspring in the next generation the  $N_{ipop}$  costs and associated individuals are ranked from lowest cost to highest cost. We retain the best  $N_{pop}$  members of the population for the next iteration of the algorithm and the rest die off. This process is called natural selection and from this point on, the size of the population at each generation is  $N_{pop}$ . Then, an equal number of mothers and fathers is selected within the  $N_{pop}$  individuals, which pair in some random fashion. There are various reasonable ways to pair individuals. A weighted cost selection with assigned probabilities is used (Haupt and Haupt, 2004). Each pair produces two offspring that contain traits from each parent. Mating is carried out by choosing one or more points in the chromosome to mark as the crossover points and the parameters between these

points are merely swapped between the two parents. In this paper a multi-point crossover operator is used and  $k_i = [1, 2, \dots, c - 1]$  crossover points are randomly selected on two individuals (parents) represented by  $c$  chromosomes. Moreover, if care is not taken, the genetic algorithm may converge too quickly into one region of the cost surface and this may be not good if the problem we are modeling has several local minima, in which the solution may get trapped. To avoid this problem of overly fast convergence, we force the routine to explore other areas of the cost surface by randomly introducing changes, or mutations, in some of the parameters. A classic mutation operator is applied to all  $N_{pop}$  individuals at each generation. For each individual  $p_i$  the mutation operator works stochastically on all the chromosomes of the individual subject to mutation (i.e. changing at random one of the individual chromosomes in the process of generating off springs). A mutation probability of 15% have been chosen.

## Structural Examples

New structural examples useful to validate the effectiveness of the GA-NURBS approach in assessing FRP reinforced masonry vaults are hereby discussed.

### Skew Arch

In the first numerical simulation, the GA-NURBS approach is applied to the case of a FRP reinforced skew circular arch, whose unreinforced version was experimentally tested in (Wang and Melbourne, 1996). The arch, named Skew 2 in (Wang and Melbourne, 1996), has a clear square span of 3000 mm, a rise of 750 mm and a skew of 45 degrees. The width of the barrel was approximately 670 mm and the average thickness 215 mm (see Fig. 1). The arch was constructed using Class A engineering bricks were on two reinforced concrete abutments representing rigid supports.

The geometry of the arch is reported in figure. In the test, a concentrated load  $P$  was applied under force control at the three quarter span mid-width of the arch barrel. An average brickwork compression strength  $f_c$  of 2.4 MPa and a tensile strength  $f_t$  of 0.2 MPa were measured, whereas a shear strength  $\tau$  of 0.1 MPa is assumed. Average specific weight of brickwork is  $22kN/m^3$ . To the aim of preventing the formation of the hinges experimentally observed in (Wang and Melbourne, 1996), we can imagine of strengthening the arch by means of two sets of FRP strips having a width of 100mm (as shown in Figure) at first only at intrados, then only at extrados and finally at both intrados and extrados. For masonry-FRP interface, a bond strength  $f_b$  equal to 0.3 MPa is assumed.

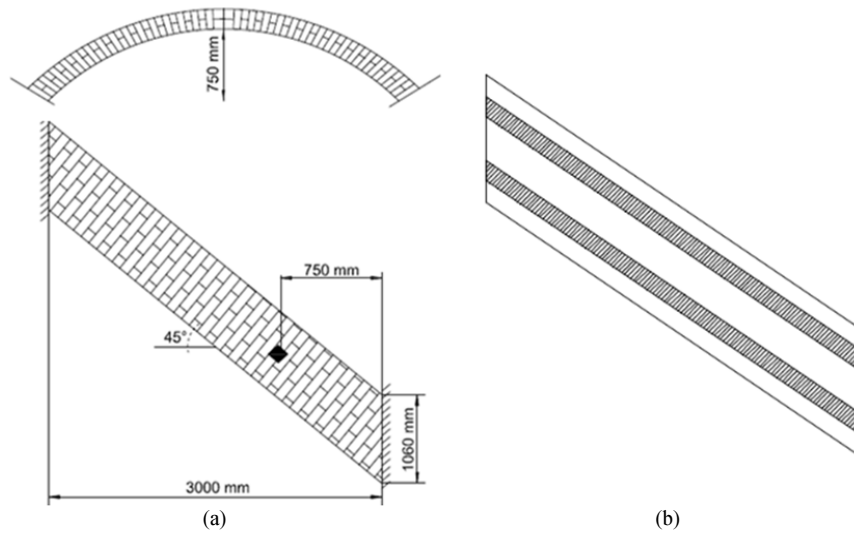


Fig. 1. (a) Skew arch geometry and loading condition; (b) FRP reinforcement disposition

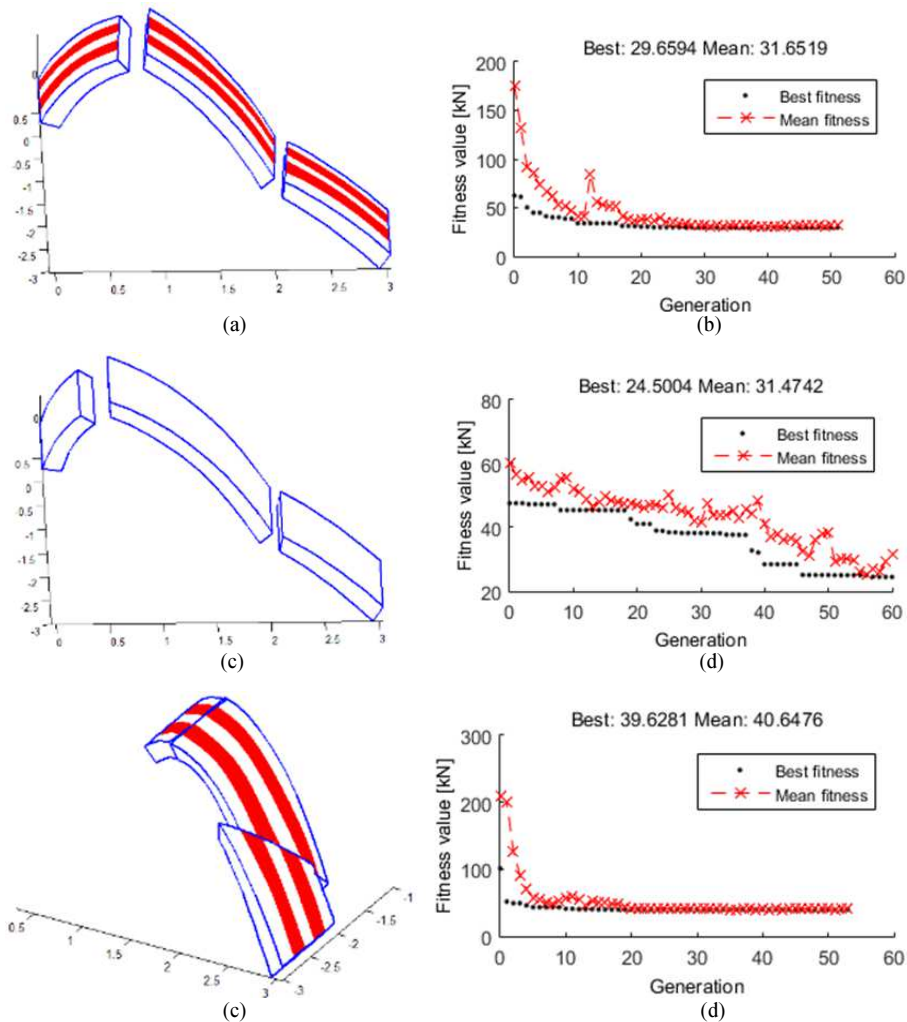


Fig. 2. Skew arch failure mechanism and convergence of the GA towards the best fitness value for different FRP dispositions: (a-b) only extrados; (c-d) only intrados; (e-f) extrados and intrados

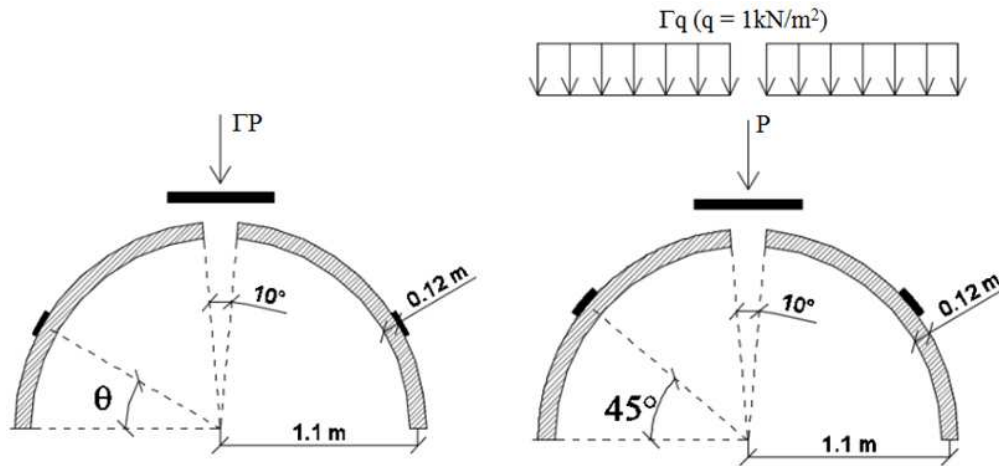


Fig. 3. Hemispherical dome geometry and FRP reinforcement disposition: (a) first load condition and (b) second load condition

The NURBS mesh of the vaulted surface is generated by two moving interfaces in the parameters space. The collapse mechanism is expected to be more complex than in a straight arch and therefore interfaces are not bounded to remain orthogonal to the shape of the arch: this means that they can rotate and, that the position of each interface in the parameters space is governed by two parameters (a translation and a rotation). Thus, the problem at hand is governed by a total of four parameters. On each interface a number of subdivisions equal to  $N_{sd} = 6$  has been chosen. In the genetic algorithm an initial population of 10 individuals have been chosen, each individual being a four element vector. A collapse load multiplier  $\lambda = 29.66$  has been obtained for the case of FRP only at extrados, whereas one gets  $\lambda = 24.50$  and  $\lambda = 39.63$  respectively for the cases of FRP only at intrados and at both intrados and extrados. The genetic algorithm allows to evaluate the optimal position of the four interfaces, in order to minimize the collapse load multiplier and therefore obtain the actual collapse mechanism for the arch. In Fig. 2(a, c, e) the respective computed collapse mechanisms are depicted. The effect of the reinforcement, which tends to counteract the formation of the hinges which cause the collapse in the unreinforced case is particularly evident, as well as the delamination of the strips, which is clearly critical near the hinges. As can be seen in Fig. 2(b, d, f), the algorithm has a fast convergence towards the optimal solution and the final best fitness value is obtained after only few generations.

### Hemispherical Dome

The second structural example here considered is an hemispherical dome with inner radius equal to 2.2m and thickness of 0.12m which was experimentally tested in (Foraboschi, 2006) for the unreinforced case with a concentrated load applied at the top. Bricks of dimensions 120×250×55 mm were used, with joints

thickness approximately equal to 10mm. Let us now consider the case of a dome reinforced with one FRP strip placed along the parallels and two different configurations for live loads: a concentrated load at the top (which simulate the presence of a roof lantern) and a uniformly distributed vertical pressure (which simulate an accidental load on the floor above the dome). An average brickwork compression strength  $f_c$  of 2.4 MPa, a tensile strength  $f_t$  of 0.2 MPa and shear strength  $\tau$  of 0.1 MPa are assumed. The optimal position of the FRP is determined through an additional genetic algorithm optimization loop acting upon the first load conditions. The so-found optimal position is then used for the second load condition. Figure 3 depicts geometry and both load conditions.

Due to the axisymmetric configuration, the NURBS mesh of the dome is generated by only one moving interface in the parameters space. This interface traces a parallel of the dome in the Euclidean space, whereas other twenty fixed interfaces in the orthogonal direction define the number of meridians subdividing the dome. Therefore, the problem at hand is governed by one parameter only. On each interface a number of  $N_{sd} = 6$  subdivisions has been chosen. In the genetic algorithm an initial population of 10 individuals has been chosen, each individual being a scalar.

Let us consider the first load condition. As shown in Fig. 4b, after design optimization of the FRP reinforcement (whose optimal position is found to be 45° latitude), a collapse load multiplier  $\lambda = 68.87$  has been obtained. Figure 4a depicts the computed collapse mechanism. As can be seen, the presence of FRP reinforcement prevents the formation of cracks along meridians and induces a shear failure of the top of the dome. Let us now consider the second load condition, with the same FRP disposition. A collapse load multiplier  $\lambda = 33.80$  has been obtained. Figure 4c depicts the computed collapse mechanism. As seen in Fig. 4d, the algorithm has a fast convergence towards the optimal solution and the final best fitness value is obtained after only few generations.

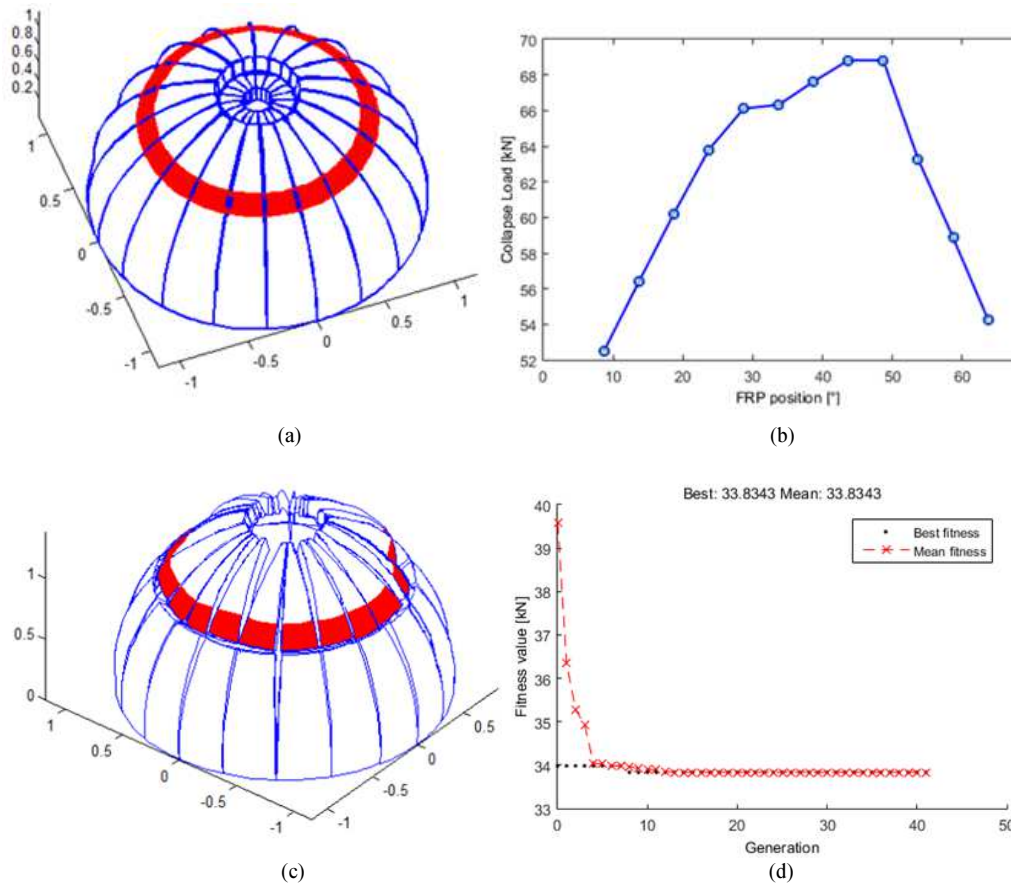


Fig. 4. Hemispherical dome: (a) collapse mechanism for the first load condition; (b) determination of the optimal position for FRP reinforcement strip; (c) collapse mechanism for the second load condition; (d) convergence of the genetic algorithm towards

### Cross Vault

As last structural example, the cross vault experimentally tested by (Faccio *et al.*, 1999) is considered. The cross vault is formed by the intersection of two barrels vaults with an external radius of 2.3m and, during experimental tests, was loaded by a vertical concentrated load at the top of the extrados of one of the border arches. Bricks of dimensions  $120 \times 250 \times 55 \text{ mm}^3$  were used, with joints thickness equal to 10 mm. Reinforcement made of FRP strips is arranged only at the extrados of the four external arches. Geometry is depicted in Fig. 5.

Two different configurations for live loads are considered (see Fig. 6-7): a concentrated load at the cross center (which simulate the presence of a heavy hanged weight) and a uniformly distributed vertical pressure upon a gravel backfill (which simulate an accidental load on the floor above the dome).

The adopted subdivision of the paramtrs space is shown in Fig. 8: due to symmetry reasons for each patch two parameters determine the position of element interfaces. Therefore, the problem at hand is governed by

eight parameters. On each interface a number of  $N_{sd} = 6$  subdivisions has been chosen. In the genetic algorithm an initial population of 10 individuals has been chosen, each individual being a twenty-four element vector.

Let us consider the first load configuration (central concentrated force). A collapse load multiplier  $\lambda = 37.91$  has been obtained. Fig. 9a shows the computed collapse mechanism. As can be seen in Fig. 9b, the algorithm has a quite fast convergence towards the optimal solution. Finally, let us consider the second load configuration (distributed vertical pressure). A collapse load multiplier  $\lambda = 18.37$  has been obtained. Fig. 9c shows the computed collapse mechanism and Fig. 9d, the convergence of the genetic algorithm towards the optimal solution.

### Conclusion

A new GA-NURBS based approach for the kinematic limit analysis of FRP reinforced masonry vaulted structures recently proposed by the authors is discussed and validated through a number of structural examples.



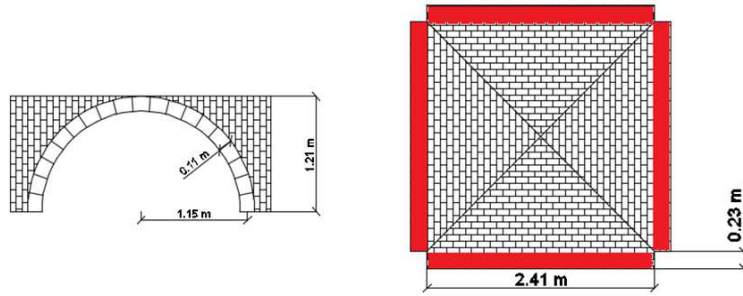


Fig. 5. Cross vault geometry and FRP disposition

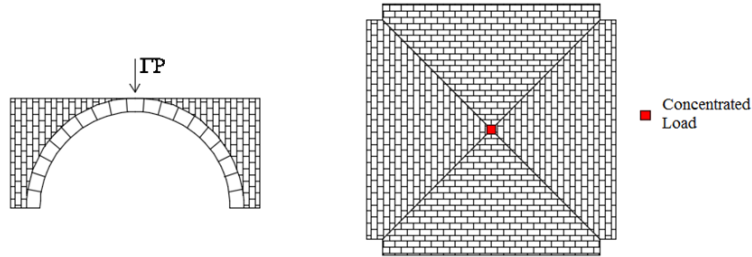


Fig. 6. First load condition: Concentrated load

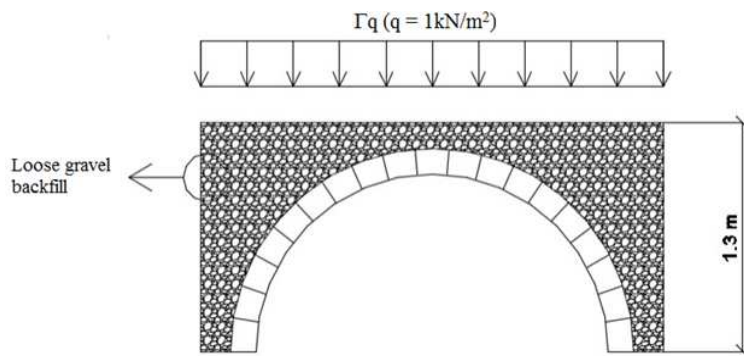


Fig. 7. Second load condition: Distributed pressure

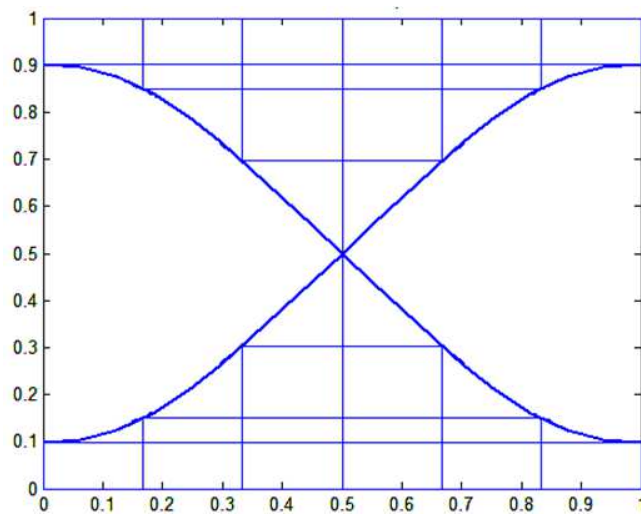


Fig. 8. Cross vault parameters space subdivision in order to obtain the rigid body assembly

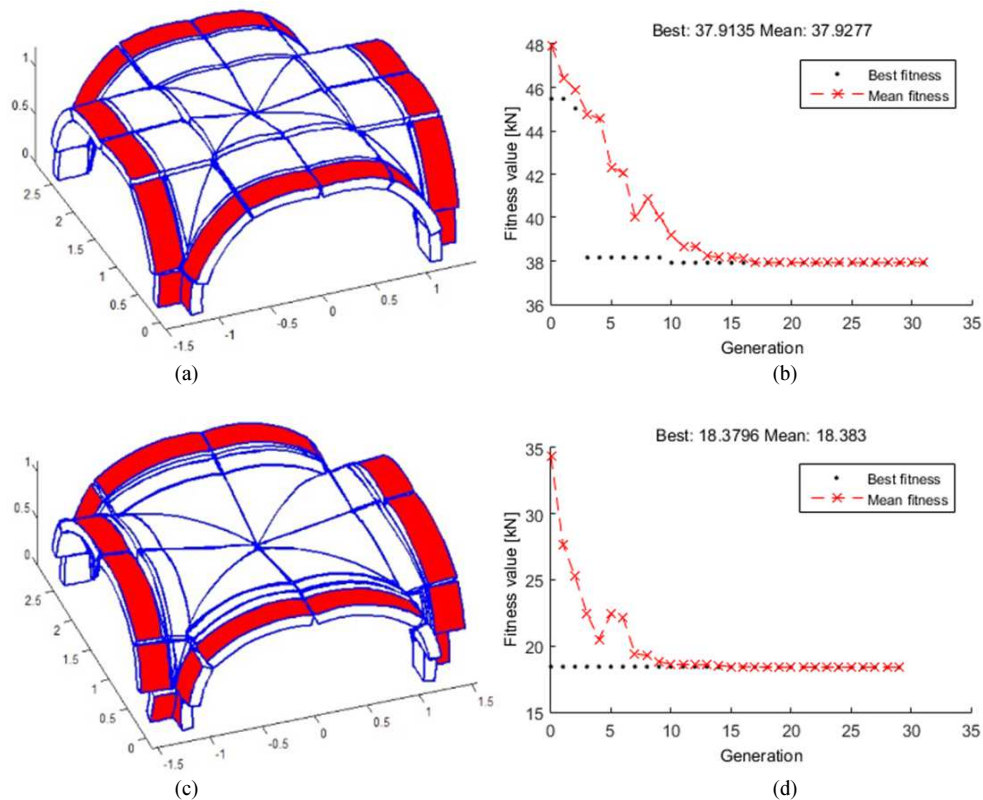


Fig. 9. Cross vault failure mechanism and convergence of the GA towards the best fitness value for different load configurations: (a-b) central concentrated force; (c-d) distributed vertical pressure

The proposed approach proves to be fast and effective in assessing load bearing capacity of FRP reinforced masonry vaults of arbitrary shape while requiring the least effort to the final user and at the same time providing good computational efficiency. The approach allows to bridge the 3D modeling environment, which is very popular among professional engineers and architects, with a structural analysis environment for FRP reinforced masonry vaults based on an upper bound limit analysis framework and proves to be a promising design tool for FRP reinforced masonry structures.

### Acknowledgement

The present investigation was developed within the activities of the (Italian) University Network of Seismic Engineering Laboratories – ReLUIS, in the research program funded by the Italian Civil Protection National Service – Research Line “Masonry Structures”, WP2-WP4.

### References

Block, P., T. Ciblac and J. Ochsendorf, 2006. Real-time limit analysis of vaulted masonry buildings. *Comput. Struct.* 84: 1841-1852.  
 DOI: 10.1016/j.compstruc.2006.08.002

Chiozzi, A., G. Milani and A. Tralli, 2016a. A Genetic Algorithm NURBS-based new approach for fast kinematic limit analysis of masonry vaults. *Comput. Struct.* Manuscript Submitted for Publication.  
 Chiozzi, A., G. Milani and A. Tralli, 2016b. Fast kinematic limit analysis of FRP-reinforced masonry vaults. II: Numerical Simulations. Manuscript Submitted for Publication.  
 Chiozzi, A., G. Milani, A. Tralli, 2016c. Fast Kinematic Limit Analysis of FRP-Reinforced Masonry Vaults. I: A General Genetic Algorithm NURBS-based Formulation. Manuscript Submitted for Publication.  
 Chiozzi, A., M. Malagù, A. Tralli and A. Cazzani, 2015. ArchNURBS: NURBS-Based Tool for the Structural Safety Assessment of Masonry Arches in MATLAB. *J. Comput. Civ. Eng.*  
 CNR-DT200, 2013. Instructions for the Design, Execution and Control of retrofit interventions on buildings by means of FRP composites (in Italian). Italian Research Council.  
 Corradi, M., A. Borri and A. Vignoli, 2002. Strengthening techniques tested on masonry structures struck by the Umbria–Marche earthquake of 1997-1998. *Constr. Build. Mater.* 16: 229-239.  
 DOI: 10.1016/S0950-0618(02)00014-4

- Cottrell, J.A., Hughes, T.J.R., Bazilevs, Y., 2009. *Isogeometric Analysis: Toward Integration of CAD and FEA*. John Wiley & Sons.
- Faccio, P., Foraboschi, P., Siviero, E., 1999. Masonry vaults reinforced with FRP strips (in italian). *L'Edilizia* 7-8, 44-50.
- Foraboschi, P., 2006. Masonry structures externally reinforced with FRP strips: tests at collapse. *Proceedings of the 1st National Conference on Experimentations on Materials and Structures (in Italian)*. Venice, Italy.
- Haupt, R.L. and S.E. Haupt, 2004. *Practical Genetic Algorithms*. John Wiley & Sons.
- McNeel, R., 2008. *Rhinoceros: Nurbs Modeling for Windows*. Robert McNeel & Associates.
- Milani, E., G. Milani and A. Tralli, 2008. Limit analysis of masonry vaults by means of curved shell finite elements and homogenization. *Int. J. Solids Struct.*, 45: 5258-5288. DOI: 10.1016/j.ijsolstr.2008.05.019
- Milani, G. and A. Tralli, 2012. A simple meso-macro model based on SQP for the non-linear analysis of masonry double curvature structures. *Int. J. Solids Struct.*, 49: 808-834.  
DOI: 10.1016/j.ijsolstr.2011.12.001
- Milani, G., E. Milani and A. Tralli, 2009. Upper Bound limit analysis model for FRP-reinforced masonry curved structures. Part I: Unreinforced masonry failure surfaces. *Comput. Struct.*, 87: 1516-1533.  
DOI: 10.1016/j.compstruc.2009.07.007
- USPRO, 1996. *Initial Graphics Exchange Specification, IGES 5.3*. U.S. Product Data Association.
- Wang, J. and C. Melbourne, 1996. *The 3-Dimensional Behaviour of Skew Masonry Arches*. The British Masonry Society. London, UK.